

CERN-EP-2022-264
21 November 2022

Enhanced deuteron coalescence probability in jets

ALICE Collaboration*

Abstract

The transverse-momentum (p_T) spectra and coalescence parameters B_2 of (anti)deuterons are measured in pp collisions at $\sqrt{s} = 13$ TeV for the first time in and out of jets. In this measurement, the direction of the leading particle with the highest p_T in the event ($p_T^{\text{lead}} > 5$ GeV/ c) is used as an approximation for the jet axis. The event is consequently divided into three azimuthal regions and the jet signal is obtained as the difference between the Toward region, that contains jet fragmentation products in addition to the underlying event (UE), and the Transverse region, which is dominated by the UE. The coalescence parameter in the jet is found to be approximately a factor of 10 larger than that in the underlying event. This experimental observation is consistent with the coalescence picture and can be attributed to the smaller average phase-space distance between nucleons in the jet cone as compared to the underlying event. The results presented in this Letter are compared to predictions from a simple nucleon coalescence model, where the phase space distributions of nucleons are generated using PYTHIA 8 with the Monash 2013 tuning, and to predictions from a deuteron production model based on ordinary nuclear reactions with parametrized energy-dependent cross sections tuned on data. The latter model is implemented in PYTHIA 8.3. Both models reproduce the observed large difference between in-jet and out-of-jet coalescence parameters, although the almost flat trend of the B_2^{jet} is not reproduced by the models, which instead give a decreasing trend.

arXiv:2211.15204v3 [nucl-ex] 8 Mar 2024

The production mechanisms of light (anti)nuclei in high-energy hadronic collisions is still unclear and currently under intense debate in the scientific community, despite the plethora of results published in recent years at different collision energies, ranging from the AGS [1–4], to the SPS [5], RHIC [6–11], and the LHC [12–27]. The experimental data are typically described using two different phenomenological approaches: the baryon coalescence approach and the statistical hadronization model (SHM). In the coalescence model [28–34], multi-baryon states are assumed to be formed by coalescence of baryons that are close in phase space at kinetic freeze-out (occurring when the elastic scatterings among the particles produced in the collision cease). In the simple coalescence approach [29], only momentum correlations are considered, while in state-of-the-art implementations [30], the quantum-mechanical properties of baryons and bound states are taken into account and the coalescence probability is calculated from the overlap between the phase-space distributions of individual (point-like) baryons and the Wigner density of the final-state cluster. The phase-space distributions of nucleons at freeze-out are generated using general-purpose Monte Carlo (MC) event generators or relativistic hydrodynamical simulations [31, 35]. In the SHM [36–43], light (anti)nuclei, as well as other hadron species, are assumed to be emitted by a source in local thermal and hadrochemical equilibrium with their abundances being fixed at chemical freeze-out (occurring when the inelastic scatterings stop). The grand-canonical approach provides an excellent description of the measured hadron yields in central nucleus–nucleus collisions, in which a large number of particles is produced, ranging from a few hundred to 2000 charged particles per unit of rapidity with increasing collision energy [40]. For small systems, such as those produced in proton–proton (pp) and proton–nucleus collisions, the production of light nuclei can be described using a different implementation of this model based on the canonical ensemble, where exact conservation of quantum numbers is required [43]. Significant deviations in this case are observed between the experimental data and the predictions from the canonical SHM [24]. The study of the production mechanisms of multi-baryon bound states in high-energy hadronic collisions is one of the goals of the experimental program of ALICE.

Measurements of light (anti)nuclei produced at accelerators are also important for indirect dark matter (DM) searches as they provide input for the estimates of the background of antinuclei produced in space. Several experiments, such as AMS-02 [44] and GAPS [45], are searching for antinuclei [46, 47], but, so far, only antiprotons have been detected in space [48]. The possible presence of antinuclei in our Galaxy could be explained either by reactions of cosmic rays (CRs) with the interstellar medium (ISM) or by decays/annihilations of dark matter candidates. Both CRs and the ISM mostly consist of hydrogen (90%), helium (8%), and only in small percentage of heavier nuclei [49]. Hence, most of the relevant collisions for the production of CR antinuclei in the Galaxy are pp, p– ^4He and ^4He –p. Antinuclei are produced if the center-of-mass energy per nucleon–nucleon collision ($\sqrt{s_{\text{NN}}}$) of such collisions is above a given energy threshold, which is 6 GeV for antideuterons and 8 GeV for anti- ^3He , for instance. Hence, one of the goals of the existing experimental programs at different accelerator facilities is to pin down the microscopic production process of antinuclei in hadronic collisions or DM decay, in order to be able to correctly interpret the future measurements in space.

Further insight into the (anti)nuclei production mechanisms can be obtained by measuring their production in and out of jets in pp collisions. Hadrons in the jet cone are closer in phase space compared with hadrons out of the jet. In a jet fragmentation, the produced particles are strongly correlated in phase space, i.e., particles which are close in space have also similar momenta [50, 51]. In the coalescence picture, this condition should result in a larger coalescence probability in jets compared with that out of jets, since the proximity in both space and momentum is required for coalescence. Hence, the probability of coalescence in jets is increased with respect to that in the UE, where space and momentum are not correlated, i.e., close-by particles can have very different momenta and vice-versa. The coalescence probability can be quantified by the coalescence parameter B_A , defined, in the case of deuterons, as the ratio between the invariant yield of the deuterons and the square of the invariant yield of protons:

$$B_2 = \left(\frac{3}{2\pi p_T^d} \frac{d^2 N_d}{dy dp_T^d} \right) / \left(\frac{3}{2\pi p_T^p} \frac{d^2 N_p}{dy dp_T^p} \right)^2, \quad (1)$$

where the labels d and p indicate the deuteron and the proton, respectively, and $p_T^p = p_T^d/2$, assuming that protons and neutrons have the same production spectra, since they belong to the same isospin doublet.

Deuteron production in jets has already been measured in pp collisions at $\sqrt{s} = 13$ TeV by the ALICE Collaboration using the two-particle correlation method [22]. The p_T spectrum of (anti)deuterons in the jet is found to be consistent with predictions based on the PYTHIA 8 event generator [52] coupled to a simple coalescence afterburner [53]. In the latter, deuteron formation is assumed to happen if a proton and a neutron have a momentum difference $\Delta p < p_0$, with $p_0 = 110$ MeV/c, thus ignoring the space coordinates in the calculation of the coalescence probability. It was also concluded that the yield of deuterons in jets, in events with a leading particle with $p_T > 5$ GeV/c at midrapidity, is about 10% of that in the underlying event (UE).

This study is expanded in this Letter and complemented by the first measurement of (anti)deuteron coalescence parameters in and out of jets. The direction of a leading particle with high transverse-momentum ($p_T^{\text{lead}} > 5$ GeV/c) at midrapidity is used as an approximation for the jet axis. The p_T spectra and coalescence parameters of (anti)deuterons are measured in three different azimuthal regions defined based on $\Delta\phi = |\phi_d - \phi_{\text{lead}}|$, where ϕ_d is the azimuthal angle of the deuterons and ϕ_{lead} is that of the leading particle. The three 120°-wide azimuthal regions and the corresponding $\Delta\phi$ intervals are the same as those defined in Refs. [54, 55]: the one around the leading particle (Toward, $|\Delta\phi| < 60^\circ$), the one back-to-back to it (Away, $|\Delta\phi| > 120^\circ$), and the one transverse to both of them (Transverse, $60^\circ < |\Delta\phi| < 120^\circ$). The Toward and Away regions contain contributions from the leading and recoil jets in addition to the underlying event, while the Transverse region is dominated by the underlying event.

A detailed description of the ALICE apparatus and its performance can be found in Refs. [56] and [57]. Trajectories of charged particles are reconstructed in the ALICE central barrel with the Inner Tracking System (ITS) [56] and the Time Projection Chamber (TPC) [58], which cover the full azimuthal angle and the pseudorapidity interval $|\eta| < 0.9$. These are located within a large solenoidal magnet, providing a highly homogeneous magnetic field of 0.5 T parallel to the beam line. The TPC provides up to 159 spatial points per track for charged-particle reconstruction and particle identification (PID) through the measurement of the specific ionization energy loss dE/dx in the gas volume. The PID is complemented by the Time-Of-Flight (TOF) system [59] located at a radial distance of 3.7 m from the nominal interaction point. It measures the arrival time of particles relative to the event collision time provided by the TOF detector itself or by the T0 detectors, two arrays of Cherenkov counters located at forward and backward rapidities ($4.6 < \eta < 4.9$ and $-3.3 < \eta < -3.0$) [57, 60].

The data used for this analysis were collected in 2016, 2017, and 2018 during the LHC pp runs at $\sqrt{s} = 13$ TeV. A minimum bias (MB) event trigger was used, which requires coincident signals in the V0 detectors (two plastic scintillator arrays located at forward and backward rapidities, $2.8 < \eta < 5.1$ and $-3.7 < \eta < -1.7$ [61]) synchronous with the bunch crossing time defined by the LHC clock. Events with multiple collision vertices, reconstructed from track segments in the two innermost layers of the ITS, are tagged as pile-up and removed from the analysis [57]. A total of approximately 1.7 billion MB pp events are considered for further analysis, corresponding to an integrated luminosity of about 30 nb^{-1} . Events with at least one charged primary particle with $p_T > 5$ GeV/c are selected, which correspond to approximately 1% of the MB pp collisions.

Deuteron candidates are selected from charged-particle tracks reconstructed in the ITS and TPC in the pseudorapidity interval $|\eta| < 0.8$. Basic track quality criteria are applied, e.g., selecting on the number of space points associated to the track in the TPC and ITS and on the χ^2 of the track fit, as done in previous light (anti)nucleus analyses, such as in Ref. [20]. The track selection criteria used for the leading particle

are the same as in Ref. [54].

(Anti)deuterons are identified in the rapidity interval $|y| < 0.5$ in the range $0.6 < p_T < 1.2$ GeV/ c by requiring that their energy loss per unit of track length measured by the TPC is within $3\sigma_{dE/dx}$ from the expected average for (anti)deuterons, where $\sigma_{dE/dx}$ is the dE/dx resolution. For $1.2 < p_T < 3.0$ GeV/ c , the particle identification is complemented by the TOF and the (anti)deuteron signal is extracted from a fit to the $n\sigma_{\text{TOF}} = (\Delta t - \Delta t_d)/\sigma_{\text{TOF}}$ distribution, where Δt is the measured time-of-flight, Δt_d its expected value for deuterons and σ_{TOF} the resolution on the time-of-flight measurement. The fit function consists of a Gaussian with an exponential tail on the right side for the signal and the sum of two exponential functions for the background [13]. The signal is extracted by integrating the signal function in the asymmetric interval $[\mu_0 - 3\sigma_{\text{TOF}}, \mu_0 + 3.5\sigma_{\text{TOF}}]$, where μ_0 is the mean of the Gaussian function.

The raw (anti)deuteron p_T spectra are corrected for the reconstruction efficiency and, only for deuterons, for the fraction of secondary deuterons produced by spallation in interactions between primary particles and the detector material. This correction is based on fits to the distance of closest approach (DCA) of the deuteron track to the primary vertex using template distributions extracted from MC simulations, as described in Refs. [20, 21, 23]. Both corrections are calculated using MC simulations in which (anti)nuclei are embedded into pp collision events generated using PYTHIA 8.1 with the Monash 2013 tune [62]. (Anti)nuclei are generated with uniform p_T and rapidity distributions within $0 < p_T < 10$ GeV/ c and $-1 < y < 1$. The passage of particles through the ALICE detector is simulated using GEANT4 [63]. The reconstruction efficiency is calculated as the ratio of the number of reconstructed and generated (anti)deuterons in the simulation, after the proper re-weighting of the generated p_T distribution according to the Lévy-Tsallis function. The same track selection and PID criteria as those used in the data are applied. The fraction of secondary deuterons is approximately 0.5 in the lowest p_T interval ($0.6 < p_T < 0.8$ GeV/ c) and decreases exponentially with increasing p_T , becoming negligible for $p_T > 1.6$ GeV/ c . The fraction of secondary deuterons is weakly dependent on the azimuthal region.

The dominant contributions to the systematic uncertainties are related to the track selection, the particle identification, the limited knowledge of the ALICE material budget, the uncertainties on the hadronic interaction cross section of (anti)deuterons, and the procedure used to estimate the fraction of secondary nuclei. The uncertainty related to the track selection is estimated by repeating the analysis using different track selection criteria and considering the RMS of the distribution of the results in each p_T interval. This contribution is found to range between 8 (1)% and 6 (5)% for deuterons (antideuterons), depending on p_T . Such uncertainty is larger for deuterons at low p_T , due to the DCA cut variations which are sensitive to the secondary nuclei. The PID uncertainty is estimated by varying the (anti)deuteron selection criteria in the TPC and TOF, the fit functions, and the signal extraction strategy (bin counting or integral of the fit function). The PID systematic uncertainty rises with p_T , from 4% to 8%. The systematic uncertainty due to the estimate of the primary fraction correction is obtained by varying the conditions (selection criteria, histogram bin width, fit range) of the fits to the DCA distributions used to estimate the correction factors. This contribution depends on the azimuthal region, and it ranges between 14% (10% and 7%) and few percent for the Away region (Toward and Transverse, respectively). The contribution from ITS–TPC and TPC–TOF matching efficiencies are estimated from charged particle tracks by comparing the probabilities of prolonging a track from the TPC to the ITS (TOF) in the data and MC [20]. The uncertainty is approximately 2% for the ITS–TPC matching efficiency and 5% for the TPC–TOF one, weakly dependent on p_T . The uncertainty on the material budget (1%) is taken from Ref. [20]. The uncertainty on the hadronic interaction cross section of (anti)deuterons is estimated by varying the default inelastic cross section of (anti)deuterons in GEANT4 by the uncertainties of the measurements [49, 64–67] and is $\sim 1\%$ (3%) for deuterons (antideuterons). The total uncertainty is obtained as the quadratic sum of each individual contribution and is found to be about 10%.

The average of the deuteron and antideuteron p_T distributions measured in the three azimuthal regions discussed above, are shown in Fig. 1 left. Individual Lévy-Tsallis fits [68] are also shown. The p_T

spectrum of (anti)deuterons in jets is obtained by subtracting the spectrum in the Transverse region, dominated by the underlying event, from that in the Toward region, which contains contributions from both jet fragmentation and the underlying event. In the subtraction, the systematic uncertainties are treated as independent, to be conservative. The resulting spectrum, with a much harder shape compared to the UE spectrum, is shown in Fig. 1 right, with squared markers, and compared to the in-jet deuteron spectrum measured with the two-particle correlation method taken from Ref. [22]. Excellent agreement is found between the deuteron p_T spectra in jets obtained with the two methods, proving the validity of the subtraction method to obtain the deuteron spectrum in jets. These results confirm that the integrated yield of deuterons in jets, in events with $p_T^{\text{lead}} > 5 \text{ GeV}/c$ at midrapidity, is only roughly 10% of that in the UE, as already pointed out in Ref. [22].

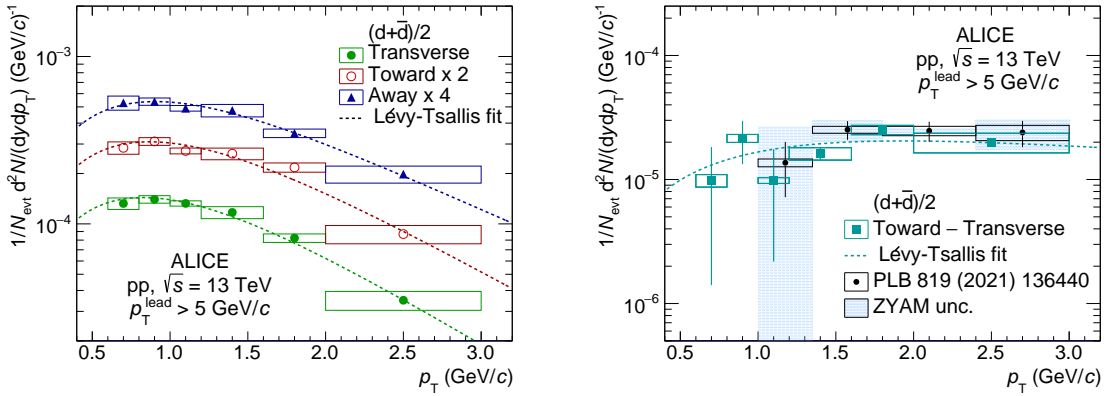


Figure 1: Average of deuteron and antideuteron p_T -differential yields in the three azimuthal regions (on the left) and in jets (on the right), measured in pp collisions at $\sqrt{s} = 13 \text{ TeV}$. Statistical and systematic uncertainties are represented by vertical bars and boxes, respectively. On the right, shaded (blue) boxes show the uncertainty on the results from Ref. [22] related to the subtraction of the uncorrelated background using the ZYAM method [69]. Individual Lévy-Tsallis fits are also shown.

The coalescence parameters in the jet (B_2^{Jet}) and underlying event (B_2^{UE}) are calculated using Eq. 1. The spectra for (anti)protons are derived from the R_T -differential p_T spectra published in Ref. [70], integrating over the full R_T , which is the underlying event activity classifier defined as $R_T = N_T^{\text{ch}} / \langle N_T^{\text{ch}} \rangle$ (N_T^{ch} being the charged-particle multiplicity measured in the Transverse region and $\langle N_T^{\text{ch}} \rangle$ its average) [54]. The p_T spectrum of (anti)protons in jets is obtained by subtracting the efficiency-corrected p_T spectra in the Transverse region from those in the Toward region taken from Ref. [70], as done for deuterons. The coalescence parameters B_2^{Jet} and B_2^{UE} are shown in Fig. 2 as a function of the transverse momentum per nucleon, p_T/A . The coalescence parameter B_2^{Jet} is found to be about a factor of 10 larger than that in the underlying event, with a significance of about 21σ . Hence, despite the limited contribution of nuclei arising from jets to their total production yield, the probability that two nucleons in the jet cone coalesce into a deuteron is enhanced with respect to the corresponding coalescence probability in the underlying event. This experimental observation can be interpreted, within the coalescence model, as due to the reduced distance in phase space between nucleons in the jets compared to those in the underlying event.

These results are compared to predictions from simple coalescence and reaction-based deuteron production models. In the former approach, the phase-space distributions of nucleons are generated with PYTHIA 8 with the Monash 2013 tune [62], and their p_T spectra are re-weighted to match the proton p_T spectra measured by ALICE in the three different azimuthal regions [70]. Spatial correlations are ignored and deuteron formation is assumed to happen if a proton and a neutron have a momentum difference below a given coalescence momentum $\Delta p < p_0$ in the deuteron rest frame. The best estimate of the coalescence momentum, for this model, is $p_0 = 285 \pm 1 \text{ MeV}/c$, which is consistent with the value of Ref. [71]. A detailed description of these coalescence calculations can be found in the Supplemental

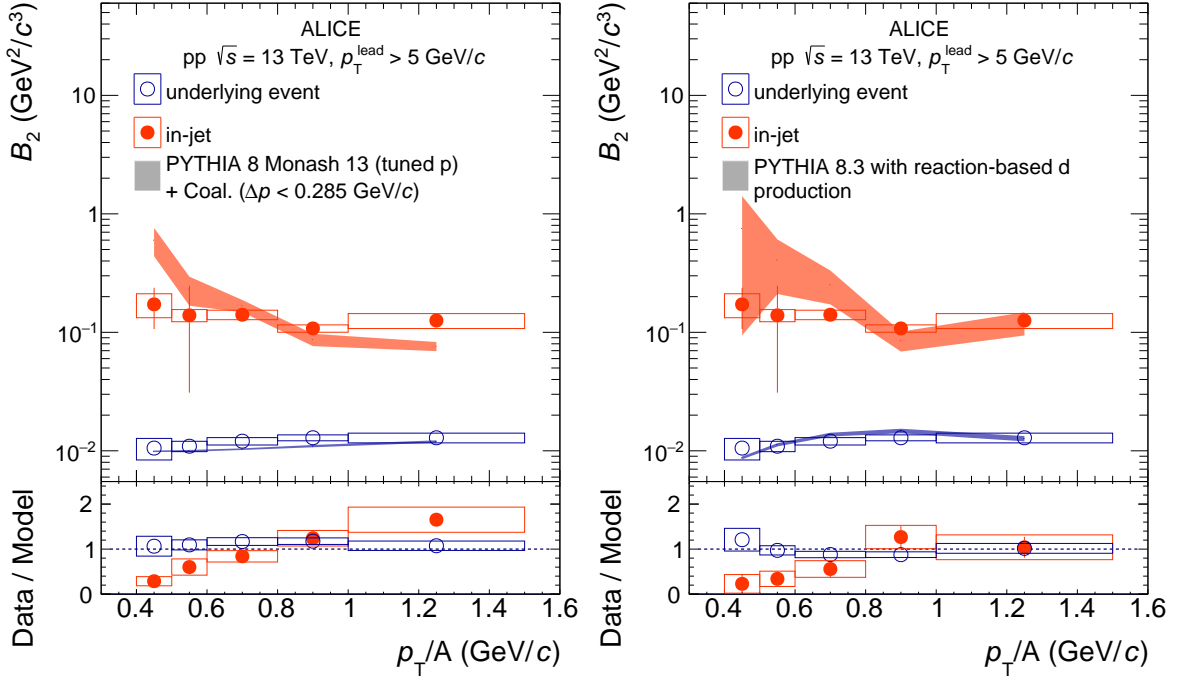


Figure 2: Coalescence parameter in jets, B_2^{Jet} , and in the underlying event, B_2^{UE} , as a function of p_T/A in comparison with the predictions from PYTHIA 8 with the Monash 2013 tune with a coalescence afterburner (left panel) and the reaction-based PYTHIA 8.3 model (right panel).

Material [72].

In the reaction-based model [73], (anti)deuterons are generated by ordinary nuclear reactions between nucleons produced in the collision with parameterized energy-dependent cross sections tuned on available experimental data [74]. The following nuclear reactions are considered: $p + n \rightarrow \gamma + d$, $p + n \rightarrow \pi^0 + d$, $p + n \rightarrow \pi^+ + \pi^- + d$, $p + n \rightarrow \pi^+ + \pi^0 + d$, $p + p \rightarrow \pi^+ + d$, $p + p \rightarrow \pi^+ + \pi^0 + d$, $n + n \rightarrow \pi^- + d$, $n + n \rightarrow \pi^- + \pi^0 + d$. Such a model is implemented in the MC event generator PYTHIA 8.3. Both simple coalescence and the reaction-based model are based on the assumption that coalescence can happen only if protons and neutrons are close in phase space. However, there are two main differences between the models. The first concerns the p_0 cut off which is introduced as a step function in the coalescence model, while in PYTHIA 8.3 the deuteron formation happens according to the differential cross section of the reactions listed above. The second difference is related to the kinematics of the process: in the coalescence model the deuteron four-momentum is given by the sum of the proton and neutron four-momenta, while in the reaction-based model, part of the initial four-momentum is carried away by the pion(s) or photon according to energy and momentum conservation rules. The uncertainties of the coalescence model are discussed in the Supplemental Material [72], while for PYTHIA 8.3 only statistical uncertainties are shown.

As shown in Fig. 2, both models provide good qualitative descriptions of the data. In particular, they are capable of reproducing the observed large difference between B_2^{Jet} and B_2^{UE} . While the p_T/A dependence of B_2^{UE} is well described by both approaches within the uncertainties, the observed nearly flat trend of B_2^{Jet} is not reproduced by the models, which instead give a decreasing trend with increasing p_T/A and overestimate the B_2^{Jet} for low p_T/A .

In this Letter the first measurement of the (anti)deuteron coalescence parameters in and out of jets in pp collisions at $\sqrt{s} = 13$ TeV is presented. The results of this work indicate for the first time an enhanced deuteron coalescence probability in jets compared to the underlying event. This enhancement, of a factor ~ 10 , is measured with a good precision and a significance of about 21σ . This experimental observation

is a parameter-free and absolute prediction of coalescence, which decisively proves the formation of bound states by coalescence when nucleons have a smaller average phase-space distance, as it is the case in the jet cone. This study will be extended to heavier (anti)nuclei, such as (anti) ^3He , and to p–Pb collisions, with the LHC Run 3 data. Further investigations of the coalescence parameters B_A in the jet and in the underlying event, in small collision systems, which reproduce the CR interactions originating nuclei in our Galaxy, will provide additional insight into the production mechanisms and will contribute to further constrain the coalescence models. These studies will be crucial to correctly interpret any future measurement of antinuclei in satellite and balloon-borne experiments in space.

Acknowledgements

The ALICE Collaboration would like to thank all its engineers and technicians for their invaluable contributions to the construction of the experiment and the CERN accelerator teams for the outstanding performance of the LHC complex. The ALICE Collaboration gratefully acknowledges the resources and support provided by all Grid centres and the Worldwide LHC Computing Grid (WLCG) collaboration. The ALICE Collaboration acknowledges the following funding agencies for their support in building and running the ALICE detector: A. I. Alikhanyan National Science Laboratory (Yerevan Physics Institute) Foundation (ANSL), State Committee of Science and World Federation of Scientists (WFS), Armenia; Austrian Academy of Sciences, Austrian Science Fund (FWF): [M 2467-N36] and Nationalstiftung für Forschung, Technologie und Entwicklung, Austria; Ministry of Communications and High Technologies, National Nuclear Research Center, Azerbaijan; Conselho Nacional de Desenvolvimento Científico e Tecnológico (CNPq), Financiadora de Estudos e Projetos (Finep), Fundação de Amparo à Pesquisa do Estado de São Paulo (FAPESP) and Universidade Federal do Rio Grande do Sul (UFRGS), Brazil; Bulgarian Ministry of Education and Science, within the National Roadmap for Research Infrastructures 2020-2027 (object CERN), Bulgaria; Ministry of Education of China (MOEC), Ministry of Science & Technology of China (MSTC) and National Natural Science Foundation of China (NSFC), China; Ministry of Science and Education and Croatian Science Foundation, Croatia; Centro de Aplicaciones Tecnológicas y Desarrollo Nuclear (CEADEN), Cubaenergía, Cuba; Ministry of Education, Youth and Sports of the Czech Republic, Czech Republic; The Danish Council for Independent Research | Natural Sciences, the VILLUM FONDEN and Danish National Research Foundation (DNRF), Denmark; Helsinki Institute of Physics (HIP), Finland; Commissariat à l’Energie Atomique (CEA) and Institut National de Physique Nucléaire et de Physique des Particules (IN2P3) and Centre National de la Recherche Scientifique (CNRS), France; Bundesministerium für Bildung und Forschung (BMBF) and GSI Helmholtzzentrum für Schwerionenforschung GmbH, Germany; General Secretariat for Research and Technology, Ministry of Education, Research and Religions, Greece; National Research, Development and Innovation Office, Hungary; Department of Atomic Energy Government of India (DAE), Department of Science and Technology, Government of India (DST), University Grants Commission, Government of India (UGC) and Council of Scientific and Industrial Research (CSIR), India; National Research and Innovation Agency - BRIN, Indonesia; Istituto Nazionale di Fisica Nucleare (INFN), Italy; Japanese Ministry of Education, Culture, Sports, Science and Technology (MEXT) and Japan Society for the Promotion of Science (JSPS) KAKENHI, Japan; Consejo Nacional de Ciencia (CONACYT) y Tecnología, through Fondo de Cooperación Internacional en Ciencia y Tecnología (FONCICYT) and Dirección General de Asuntos del Personal Académico (DGAPA), Mexico; Nederlandse Organisatie voor Wetenschappelijk Onderzoek (NWO), Netherlands; The Research Council of Norway, Norway; Commission on Science and Technology for Sustainable Development in the South (COMSATS), Pakistan; Pontificia Universidad Católica del Perú, Peru; Ministry of Education and Science, National Science Centre and WUT ID-UB, Poland; Korea Institute of Science and Technology Information and National Research Foundation of Korea (NRF), Republic of Korea; Ministry of Education and Scientific Research, Institute of Atomic Physics, Ministry of Research and Innovation and Institute of Atomic Physics and University Politehnica of Bucharest, Romania; Ministry of Education, Science, Research and Sport of

the Slovak Republic, Slovakia; National Research Foundation of South Africa, South Africa; Swedish Research Council (VR) and Knut & Alice Wallenberg Foundation (KAW), Sweden; European Organization for Nuclear Research, Switzerland; Suranaree University of Technology (SUT), National Science and Technology Development Agency (NSTDA), Thailand Science Research and Innovation (TSRI) and National Science, Research and Innovation Fund (NSRF), Thailand; Turkish Energy, Nuclear and Mineral Research Agency (TENMAK), Turkey; National Academy of Sciences of Ukraine, Ukraine; Science and Technology Facilities Council (STFC), United Kingdom; National Science Foundation of the United States of America (NSF) and United States Department of Energy, Office of Nuclear Physics (DOE NP), United States of America. In addition, individual groups or members have received support from: Marie Skłodowska Curie, European Research Council, Strong 2020 - Horizon 2020 (grant nos. 950692, 824093, 896850), European Union; Academy of Finland (Center of Excellence in Quark Matter) (grant nos. 346327, 346328), Finland; Programa de Apoyos para la Superación del Personal Académico, UNAM, Mexico.

References

- [1] **E878** Collaboration, M. J. Bennett *et al.*, “Light nuclei production in relativistic Au + nucleus collisions”, *Phys. Rev. C* **58** (1998) 1155–1164.
- [2] **E802** Collaboration, L. Ahle *et al.*, “Proton and deuteron production in Au + Au reactions at 11.6 A-GeV/c”, *Phys. Rev. C* **60** (1999) 064901.
- [3] **E864** Collaboration, T. A. Armstrong *et al.*, “Measurements of light nuclei production in 11.5 A-GeV/c Au + Pb heavy ion collisions”, *Phys. Rev. C* **61** (2000) 064908, arXiv:nuc1-ex/0003009.
- [4] **E864** Collaboration, T. A. Armstrong *et al.*, “Anti-deuteron yield at the AGS and coalescence implications”, *Phys. Rev. Lett.* **85** (2000) 2685–2688, arXiv:nuc1-ex/0005001.
- [5] **NA52 (NEWMASS)** Collaboration, G. Ambrosini *et al.*, “Baryon and anti-baryon production in lead-lead collisions at 158 A GeV/c”, *Phys. Lett. B* **417** (1998) 202–210.
- [6] **STAR** Collaboration, C. Adler *et al.*, “Antideuteron and anti-³He production in $\sqrt{s_{NN}} = 130$ GeV Au+Au collisions”, *Phys. Rev. Lett.* **87** (2001) 262301, arXiv:nuc1-ex/0108022. [Erratum: *Phys.Rev.Lett.* **87**, 279902 (2001)].
- [7] **PHENIX** Collaboration, S. S. Adler *et al.*, “Deuteron and antideuteron production in Au + Au collisions at 200 GeV”, *Phys. Rev. Lett.* **94** (2005) 122302, arXiv:nuc1-ex/0406004.
- [8] **BRAHMS** Collaboration, I. Arsene *et al.*, “Rapidity dependence of deuteron production in Au+Au collisions at $\sqrt{s_{NN}} = 200$ GeV”, *Phys. Rev. C* **83** (2011) 044906, arXiv:1005.5427 [nuc1-ex].
- [9] **STAR** Collaboration, H. Agakishiev *et al.*, “Observation of the antimatter helium-4 nucleus”, *Nature* **473** (2011) 353, arXiv:1103.3312 [nuc1-ex]. [Erratum: *Nature* **475** (2011) 412].
- [10] **STAR** Collaboration, L. Adamczyk *et al.*, “Measurement of elliptic flow of light nuclei at $\sqrt{s_{NN}} = 200, 62.4, 39, 27, 19.6, 11.5,$ and 7.7 GeV at the BNL Relativistic Heavy Ion Collider”, *Phys. Rev. C* **94** (2016) 034908, arXiv:1601.07052 [nuc1-ex].
- [11] **STAR** Collaboration, J. Adam *et al.*, “Beam energy dependence of (anti-)deuteron production in Au + Au collisions at the BNL Relativistic Heavy Ion Collider”, *Phys. Rev. C* **99** (2019) 064905, arXiv:1903.11778 [nuc1-ex].
- [12] **ALICE** Collaboration, J. Adam *et al.*, “Precision measurement of the mass difference between light nuclei and anti-nuclei”, *Nature Phys.* **11** (2015) 811–814, arXiv:1508.03986 [nuc1-ex].

- [13] **ALICE** Collaboration, J. Adam *et al.*, “Production of light nuclei and anti-nuclei in pp and Pb–Pb collisions at energies available at the CERN Large Hadron Collider”, *Phys. Rev.* **C93** (2016) 024917, arXiv:1506.08951 [nucl-ex].
- [14] **ALICE** Collaboration, S. Acharya *et al.*, “Multiplicity dependence of (anti-)deuteron production in pp collisions at $\sqrt{s} = 7$ TeV”, *Phys. Lett.* **B794** (2019) 50–63, arXiv:1902.09290 [nucl-ex].
- [15] **ALICE** Collaboration, S. Acharya *et al.*, “Measurement of deuteron spectra and elliptic flow in Pb–Pb collisions at $\sqrt{s_{NN}} = 2.76$ TeV at the LHC”, *Eur. Phys. J.* **C77** (2017) 658, arXiv:1707.07304 [nucl-ex].
- [16] **ALICE** Collaboration, S. Acharya *et al.*, “Production of deuterons, tritons, ^3He nuclei and their antinuclei in pp collisions at $\sqrt{s} = 0.9, 2.76$ and 7 TeV”, *Phys. Rev.* **C97** (2018) 024615, arXiv:1709.08522 [nucl-ex].
- [17] **ALICE** Collaboration, S. Acharya *et al.*, “Production of ^4He and $^4\overline{\text{He}}$ in Pb–Pb collisions at $\sqrt{s_{NN}} = 2.76$ TeV at the LHC”, *Nucl. Phys.* **A971** (2018) 1–20, arXiv:1710.07531 [nucl-ex].
- [18] **ALICE** Collaboration, S. Acharya *et al.*, “Multiplicity dependence of light (anti-)nuclei production in p–Pb collisions at $\sqrt{s_{NN}} = 5.02$ TeV”, *Phys. Lett. B* **800** (2020) 135043, arXiv:1906.03136 [nucl-ex].
- [19] **ALICE** Collaboration, S. Acharya *et al.*, “Production of (anti-) ^3He and (anti-) ^3H in p–Pb collisions at $\sqrt{s_{NN}} = 5.02$ TeV”, *Phys. Rev.* **C101** (2020) 044906, arXiv:1910.14401 [nucl-ex].
- [20] **ALICE** Collaboration, S. Acharya *et al.*, “(Anti-)deuteron production in pp collisions at $\sqrt{s} = 13$ TeV”, *Eur. Phys. J. C* **80** (2020) 889, arXiv:2003.03184 [nucl-ex].
- [21] **ALICE** Collaboration, S. Acharya *et al.*, “Production of light (anti)nuclei in pp collisions at $\sqrt{s} = 13$ TeV”, *JHEP* **01** (2022) 106, arXiv:2109.13026 [nucl-ex].
- [22] **ALICE** Collaboration, S. Acharya *et al.*, “Jet-associated deuteron production in pp collisions at $\sqrt{s} = 13$ TeV”, *Phys. Lett. B* **819** (2021) 136440, arXiv:2011.05898 [nucl-ex].
- [23] **ALICE** Collaboration, S. Acharya *et al.*, “Production of light (anti)nuclei in pp collisions at $\sqrt{s} = 5.02$ TeV”, *Eur. Phys. J. C* **82** (2022) 289, arXiv:2112.00610 [nucl-ex].
- [24] **ALICE** Collaboration, S. Acharya *et al.*, “Hypertriton Production in p–Pb Collisions at $\sqrt{s_{NN}}=5.02$ TeV”, *Phys. Rev. Lett.* **128** (2022) 252003, arXiv:2107.10627 [nucl-ex].
- [25] **ALICE** Collaboration, S. Acharya *et al.*, “Measurement of deuteron spectra and elliptic flow in Pb–Pb collisions at $\sqrt{s_{NN}} = 2.76$ TeV at the LHC”, *Eur. Phys. J. C* **77** (2017) 658, arXiv:1707.07304 [nucl-ex].
- [26] **ALICE** Collaboration, S. Acharya *et al.*, “Elliptic and triangular flow of (anti)deuterons in Pb–Pb collisions at $\sqrt{s_{NN}} = 5.02$ TeV”, *Phys. Rev. C* **102** (2020) 055203, arXiv:2005.14639 [nucl-ex].
- [27] **ALICE** Collaboration, S. Acharya *et al.*, “Measurement of the (anti-) ^3He elliptic flow in Pb–Pb collisions at $\sqrt{s_{NN}} = 5.02$ TeV”, *Phys. Lett. B* **805** (2020) 135414, arXiv:1910.09718 [nucl-ex].
- [28] S. T. Butler and C. A. Pearson, “Deuterons from High-Energy Proton Bombardment of Matter”, *Phys. Rev.* **129** (1963) 836–842.

- [29] J. I. Kapusta, “Mechanisms for deuteron production in relativistic nuclear collisions”, *Phys. Rev. C* **21** (1980) 1301–1310.
- [30] R. Scheibl and U. W. Heinz, “Coalescence and flow in ultrarelativistic heavy ion collisions”, *Phys. Rev. C* **59** (1999) 1585–1602, arXiv:nuc1-th/9809092 [nucl-th].
- [31] W. Zhao, L. Zhu, H. Zheng, C. M. Ko, and H. Song, “Spectra and flow of light nuclei in relativistic heavy ion collisions at energies available at the BNL Relativistic Heavy Ion Collider and at the CERN Large Hadron Collider”, *Phys. Rev. C* **98** (2018) 054905, arXiv:1807.02813 [nucl-th].
- [32] K. Blum and M. Takimoto, “Nuclear coalescence from correlation functions”, *Phys. Rev. C* **99** (2019) 044913, arXiv:1901.07088 [nucl-th].
- [33] K.-J. Sun, C. M. Ko, and B. Dönigus, “Suppression of light nuclei production in collisions of small systems at the Large Hadron Collider”, *Phys. Lett. B* **792** (2019) 132–137, arXiv:1812.05175 [nucl-th].
- [34] M. Kachelrieß, S. Ostapchenko, and J. Tjemsland, “Alternative coalescence model for deuteron, tritium, helium-3 and their antinuclei”, *Eur. Phys. J. A* **56** (2020) 4, arXiv:1905.01192 [hep-ph].
- [35] D. Oliinychenko, L.-G. Pang, H. Elfner, and V. Koch, “Microscopic study of deuteron production in Pb–Pb collisions at $\sqrt{s_{NN}} = 2.76$ TeV via hydrodynamics and a hadronic afterburner”, *Phys. Rev. C* **99** (2019) 044907, arXiv:1809.03071 [hep-ph].
- [36] J. Cleymans, S. Kabana, I. Kraus, H. Oeschler, K. Redlich, and N. Sharma, “Antimatter production in proton-proton and heavy-ion collisions at ultrarelativistic energies”, *Phys. Rev. C* **84** (2011) 054916, arXiv:1105.3719 [hep-ph].
- [37] A. Andronic, P. Braun-Munzinger, J. Stachel, and H. Stöcker, “Production of light nuclei, hypernuclei and their antiparticles in relativistic nuclear collisions”, *Phys. Lett. B* **697** (2011) 203–207, arXiv:1010.2995 [nucl-th].
- [38] F. Becattini, E. Grossi, M. Bleicher, J. Steinheimer, and R. Stock, “Centrality dependence of hadronization and chemical freeze-out conditions in heavy ion collisions at $\sqrt{s_{NN}} = 2.76$ TeV”, *Phys. Rev. C* **90** (2014) 054907, arXiv:1405.0710 [nucl-th].
- [39] V. Vovchenko and H. Stöcker, “Examination of the sensitivity of the thermal fits to heavy-ion hadron yield data to the modeling of the eigenvolume interactions”, *Phys. Rev. C* **95** (2017) 044904, arXiv:1606.06218 [hep-ph].
- [40] A. Andronic, P. Braun-Munzinger, K. Redlich, and J. Stachel, “Decoding the phase structure of QCD via particle production at high energy”, *Nature* **561** (2018) 321–330, arXiv:1710.09425 [nucl-th].
- [41] N. Sharma, J. Cleymans, B. Hippolyte, and M. Paradza, “A Comparison of p-p, p-Pb, Pb-Pb Collisions in the Thermal Model: Multiplicity Dependence of Thermal Parameters”, *Phys. Rev. C* **99** (2019) 044914, arXiv:1811.00399 [hep-ph].
- [42] V. Vovchenko, B. Dönigus, and H. Stoecker, “Canonical statistical model analysis of p-p, p-Pb, and Pb–Pb collisions at energies available at the CERN Large Hadron Collider”, *Phys. Rev. C* **100** (2019) 054906, arXiv:1906.03145 [hep-ph].
- [43] V. Vovchenko, B. Dönigus, and H. Stoecker, “Multiplicity dependence of light nuclei production at LHC energies in the canonical statistical model”, *Phys. Lett. B* **785** (2018) 171–174, arXiv:1808.05245 [hep-ph].

- [44] A. Kounine, “The Alpha Magnetic Spectrometer on the International Space Station”, *Int. J. Mod. Phys. E* **21** (2012) 1230005.
- [45] C. J. Hailey, “An indirect search for dark matter using antideuterons: the GAPS experiment”, *New J. Phys.* **11** (2009) 105022.
- [46] F. Donato, N. Fornengo, and D. Maurin, “Antideuteron fluxes from dark matter annihilation in diffusion models”, *Phys. Rev.* **D78** (2008) 043506, arXiv:0803.2640 [hep-ph].
- [47] M. Korsmeier, F. Donato, and N. Fornengo, “Prospects to verify a possible dark matter hint in cosmic antiprotons with antideuterons and antihelium”, *Phys. Rev.* **D97** (2018) 103011, arXiv:1711.08465 [astro-ph.HE].
- [48] AMS Collaboration, M. Aguilar *et al.*, “Antiproton Flux, Antiproton-to-Proton Flux Ratio, and Properties of Elementary Particle Fluxes in Primary Cosmic Rays Measured with the Alpha Magnetic Spectrometer on the International Space Station”, *Phys. Rev. Lett.* **117** (2016) 091103.
- [49] ALICE Collaboration, S. Acharya *et al.*, “Measurement of the low-energy antideuteron inelastic cross section”, *Phys. Rev. Lett.* **125** (2020) 162001, arXiv:2005.11122 [nucl-ex].
- [50] R. D. Field and R. P. Feynman, “A Parametrization of the Properties of Quark Jets”, *Nucl. Phys. B* **136** (1978) 1.
- [51] B. Andersson, G. Gustafson, G. Ingelman, and T. Sjostrand, “Parton Fragmentation and String Dynamics”, *Phys. Rept.* **97** (1983) 31–145.
- [52] T. Sjostrand, S. Mrenna, and P. Z. Skands, “A Brief Introduction to PYTHIA 8.1”, *Comput. Phys. Commun.* **178** (2008) 852–867, arXiv:0710.3820 [hep-ph].
- [53] ALICE Collaboration, S. Acharya *et al.*, “Supplemental material: afterburner for generating light (anti-)nuclei with QCD-inspired event generators in pp collisions”, *ALICE-PUBLIC-2017-010* (Sep, 2017). <https://cds.cern.ch/record/2285500>.
- [54] ALICE Collaboration, S. Acharya *et al.*, “Underlying Event properties in pp collisions at $\sqrt{s} = 13$ TeV”, *JHEP* **04** (2020) 192, arXiv:1910.14400 [nucl-ex].
- [55] ALICE Collaboration, “Underlying-event properties in pp and p–Pb collisions at $\sqrt{s_{NN}} = 5.02$ TeV”, *JHEP* **06** (2023) 023, arXiv:2204.10389 [nucl-ex].
- [56] ALICE Collaboration, K. Aamodt *et al.*, “The ALICE experiment at the CERN LHC”, *JINST* **3** (2008) S08002. <https://iopscience.iop.org/article/10.1088/1748-0221/3/08/S08002>.
- [57] ALICE Collaboration, B. Abelev *et al.*, “Performance of the ALICE Experiment at the CERN LHC”, *Int. J. Mod. Phys.* **A29** (2014) 1430044, arXiv:1402.4476 [nucl-ex].
- [58] J. Alme *et al.*, “The ALICE TPC, a large 3-dimensional tracking device with fast readout for ultra-high multiplicity events”, *Nucl. Instrum. Meth.* **A622** (2010) 316–367, arXiv:1001.1950 [physics.ins-det].
- [59] ALICE Collaboration, A. Akindinov *et al.*, “Performance of the ALICE Time-Of-Flight detector at the LHC”, *Eur. Phys. J. Plus* **128** (2013) 44.
- [60] ALICE Collaboration, J. Adam *et al.*, “Determination of the event collision time with the ALICE detector at the LHC”, *Eur. Phys. J. Plus* **132** (2017) 99, arXiv:1610.03055 [physics.ins-det].









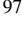


- [61] **ALICE** Collaboration, P. Cortese *et al.*, “ALICE technical design report on forward detectors: FMD, T0 and V0”, (2004) CERN–LHCC–2004–025.
- [62] P. Skands *et al.*, “Tuning PYTHIA 8.1: the Monash 2013 Tune”, *Eur. Phys. J. C* **74** (2014) 3024, arXiv:1404.5630 [hep-ph].
- [63] **GEANT4** Collaboration, S. Agostinelli *et al.*, “GEANT4—a simulation toolkit”, *Nucl. Instrum. Meth. A* **506** (2003) 250–303.
- [64] J. Jaros *et al.*, “Nucleus-nucleus total cross sections for light nuclei at 1.55 and 2.89 GeV/c per nucleon”, *Phys. Rev. C* **18** (1978) 2273–2292.
- [65] A. Auce *et al.*, “Reaction cross sections for 38, 65, and 97 MeV deuterons on targets from ${}^9\text{Be}$ to ${}^{208}\text{Pb}$ ”, *Phys. Rev. C* **53** (1996) 2919–2925.
- [66] S. P. Denisov *et al.*, “Measurements of anti-deuteron absorption and stripping cross sections at the momentum 13.3 GeV/c”, *Nucl. Phys. B* **31** (1971) 253–260.
- [67] F. G. Binon *et al.*, “Absorption cross-sections of 25 GeV/c antideuterons in Li, C, Al, Cu and Pb”, *Phys. Lett. B* **31** (1970) 230–232.
- [68] C. Tsallis, “Possible Generalization of Boltzmann-Gibbs Statistics”, *J. Statist. Phys.* **52** (1988) 479–487.
- [69] **PHENIX** Collaboration, S. S. Adler *et al.*, “Dense-Medium Modifications to Jet-Induced Hadron Pair Distributions in Au+Au Collisions at $\sqrt{s_{\text{NN}}} = 200$ GeV”, *Phys. Rev. Lett.* **97** (2006) 052301, arXiv:nucl-ex/0507004.
- [70] **ALICE** Collaboration, “Production of pions, kaons and protons as a function of the transverse event activity in pp collisions at $\sqrt{s} = 13$ TeV”, *JHEP* **06** (2023) 027, arXiv:2301.10120 [nucl-ex].
- [71] S. Sombun *et al.*, “Deuteron production from phase-space coalescence in the UrQMD approach”, *Phys. Rev. C* **99** (2019) 014901, arXiv:1805.11509 [nucl-th].
- [72] **ALICE** Collaboration, “Enhanced deuteron coalescence probability in jets. Supplemental Material: a model based on PYTHIA 8 and simple nucleon coalescence”, *ALICE-PUBLIC-2022-019* (Nov, 2022) . <http://cds.cern.ch/record/2842026>.
- [73] C. Bierlich *et al.*, “A comprehensive guide to the physics and usage of PYTHIA 8.3”, arXiv:2203.11601 [hep-ph].
- [74] L. A. Dal and A. R. Raklev, “Alternative formation model for antideuterons from dark matter”, *Phys. Rev. D* **91** (2015) 123536, arXiv:1504.07242 [hep-ph]. [Erratum: *Phys.Rev.D* **92**, 069903 (2015), Erratum: *Phys.Rev.D* **92**, 089901 (2015)].

A The ALICE Collaboration

S. Acharya ¹²⁵, D. Adamová ⁸⁶, A. Adler⁶⁹, G. Aglieri Rinella ³², M. Agnello ²⁹, N. Agrawal ⁵⁰, Z. Ahammed ¹³², S. Ahmad ¹⁵, S.U. Ahn ⁷⁰, I. Ahuja ³⁷, A. Akindinov ¹⁴⁰, M. Al-Turany ⁹⁷, D. Aleksandrov ¹⁴⁰, B. Alessandro ⁵⁵, H.M. Alfanda ⁶, R. Alfaro Molina ⁶⁶, B. Ali ¹⁵, A. Alici ²⁵, N. Alizadehvandchali ¹¹⁴, A. Alkin ³², J. Alme ²⁰, G. Alocco ⁵¹, T. Alt ⁶³, I. Altsybeev ¹⁴⁰, M.N. Anaam ⁶, C. Andrei ⁴⁵, A. Andronic ¹³⁵, V. Anguelov ⁹⁴, F. Antinori ⁵³, P. Antonioli ⁵⁰, N. Apadula ⁷⁴, L. Aphecetche ¹⁰³, H. Appelshäuser ⁶³, C. Arata ⁷³, S. Arcelli ²⁵, M. Aresti ⁵¹, R. Arnaldi ⁵⁵, J.G.M.C.A. Arneiro ¹¹⁰, I.C. Arsene ¹⁹, M. Arslanok ¹³⁷, A. Augustinus ³², R. Averbeck ⁹⁷, M.D. Azmi ¹⁵, A. Badalà ⁵², J. Bae ¹⁰⁴, Y.W. Baek ⁴⁰, X. Bai ¹¹⁸, R. Bailhache ⁶³, Y. Bailung ⁴⁷, A. Balbino ²⁹, A. Baldisseri ¹²⁸, B. Balis ², D. Banerjee ⁴, Z. Banoo ⁹¹, R. Barbera ²⁶, F. Barile ³¹, L. Barioglio ⁹⁵, M. Barlou⁷⁸, G.G. Barnaföldi ¹³⁶, L.S. Barnby ⁸⁵, V. Barret ¹²⁵, L. Barreto ¹¹⁰, C. Bartels ¹¹⁷, K. Barth ³², E. Bartsch ⁶³, N. Bastid ¹²⁵, S. Basu ⁷⁵, G. Batigne ¹⁰³, D. Battistini ⁹⁵, B. Batyunya ¹⁴¹, D. Bauri⁴⁶, J.L. Bazo Alba ¹⁰¹, I.G. Bearden ⁸³, C. Beattie ¹³⁷, P. Becht ⁹⁷, D. Behera ⁴⁷, I. Belikov ¹²⁷, A.D.C. Bell Hechavarria ¹³⁵, F. Bellini ²⁵, R. Bellwied ¹¹⁴, S. Belokurova ¹⁴⁰, V. Belyaev ¹⁴⁰, G. Bencedi ¹³⁶, S. Beole ²⁴, A. Bercuci ⁴⁵, Y. Berdnikov ¹⁴⁰, A. Berdnikova ⁹⁴, L. Bergmann ⁹⁴, M.G. Besoiu ⁶², L. Betev ³², P.P. Bhaduri ¹³², A. Bhasin ⁹¹, M.A. Bhat ⁴, B. Bhattacharjee ⁴¹, L. Bianchi ²⁴, N. Bianchi ⁴⁸, J. Bielčik ³⁵, J. Bielčiková ⁸⁶, J. Biernat ¹⁰⁷, A.P. Bigot ¹²⁷, A. Bilandzic ⁹⁵, G. Biro ¹³⁶, S. Biswas ⁴, N. Bize ¹⁰³, J.T. Blair ¹⁰⁸, D. Blau ¹⁴⁰, M.B. Blidaru ⁹⁷, N. Bluhme³⁸, C. Blume ⁶³, G. Boca ^{21,54}, F. Bock ⁸⁷, T. Bodova ²⁰, A. Bogdanov¹⁴⁰, S. Boi ²², J. Bok ⁵⁷, L. Boldizsár ¹³⁶, A. Bolozdynya ¹⁴⁰, M. Bombara ³⁷, P.M. Bond ³², G. Bonomi ^{131,54}, H. Borel ¹²⁸, A. Borissov ¹⁴⁰, A.G. Borquez Carcamo ⁹⁴, H. Bossi ¹³⁷, E. Botta ²⁴, Y.E.M. Bouziani ⁶³, L. Bratrud ⁶³, P. Braun-Munzinger ⁹⁷, M. Bregant ¹¹⁰, M. Broz ³⁵, G.E. Bruno ^{96,31}, M.D. Buckland ²³, D. Budnikov ¹⁴⁰, H. Buesching ⁶³, S. Bufalino ²⁹, O. Bugnon¹⁰³, P. Buhler ¹⁰², Z. Buthelezi ^{67,121}, S.A. Bysiak¹⁰⁷, M. Cai ⁶, H. Caines ¹³⁷, A. Caliva ⁹⁷, E. Calvo Villar ¹⁰¹, J.M.M. Camacho ¹⁰⁹, P. Camerini ²³, F.D.M. Canedo ¹¹⁰, M. Carabas ¹²⁴, A.A. Carballo ³², F. Carnesecchi ³², R. Caron ¹²⁶, L.A.D. Carvalho ¹¹⁰, J. Castillo Castellanos ¹²⁸, F. Catalano ^{24,29}, C. Ceballos Sanchez ¹⁴¹, I. Chakaberia ⁷⁴, P. Chakraborty ⁴⁶, S. Chandra ¹³², S. Chapeland ³², M. Chartier ¹¹⁷, S. Chattopadhyay ¹³², S. Chattopadhyay ⁹⁹, T.G. Chavez ⁴⁴, T. Cheng ^{97,6}, C. Cheshkov ¹²⁶, B. Cheynis ¹²⁶, V. Chibante Barroso ³², D.D. Chinellato ¹¹¹, E.S. Chizzali ^{11,95}, J. Cho ⁵⁷, S. Cho ⁵⁷, P. Chochula ³², P. Christakoglou ⁸⁴, C.H. Christensen ⁸³, P. Christiansen ⁷⁵, T. Chujo ¹²³, M. Ciacco ²⁹, C. Cicalo ⁵¹, F. Cindolo ⁵⁰, M.R. Ciupek⁹⁷, G. Clai^{III,50}, F. Colamaria ⁴⁹, J.S. Colburn¹⁰⁰, D. Colella ^{96,31}, M. Colocci ³², M. Concas ^{IV,55}, G. Conesa Balbastre ⁷³, Z. Conesa del Valle ⁷², G. Contin ²³, J.G. Contreras ³⁵, M.L. Coquet ¹²⁸, T.M. Cormier^{I,87}, P. Cortese ^{130,55}, M.R. Cosentino ¹¹², F. Costa ³², S. Costanza ^{21,54}, C. Cot ⁷², J. Crkovská ⁹⁴, P. Crochet ¹²⁵, R. Cruz-Torres ⁷⁴, E. Cuautle⁶⁴, P. Cui ⁶, A. Dainese ⁵³, M.C. Danisch ⁹⁴, A. Danu ⁶², P. Das ⁸⁰, P. Das ⁴, S. Das ⁴, A.R. Dash ¹³⁵, S. Dash ⁴⁶, R.M.H. David⁴⁴, A. De Caro ²⁸, G. de Cataldo ⁴⁹, J. de Cuveland³⁸, A. De Falco ²², D. De Gruttola ²⁸, N. De Marco ⁵⁵, C. De Martin ²³, S. De Pasquale ²⁸, S. Deb ⁴⁷, R.J. Debski ², K.R. Deja¹³³, R. Del Grande ⁹⁵, L. Dello Stritto ²⁸, W. Deng ⁶, P. Dhankher ¹⁸, D. Di Bari ³¹, A. Di Mauro ³², R.A. Diaz ^{141,7}, T. Dietel ¹¹³, Y. Ding ^{126,6}, R. Divià ³², D.U. Dixit ¹⁸, Ø. Djuvsland²⁰, U. Dmitrieva ¹⁴⁰, A. Dobrin ⁶², B. Dönigus ⁶³, J.M. Dubinski ¹³³, A. Dubla ⁹⁷, S. Dudi ⁹⁰, P. Dupieux ¹²⁵, M. Durkac¹⁰⁶, N. Dzalaiova¹², T.M. Eder ¹³⁵, R.J. Ehlers ⁸⁷, V.N. Eikeland²⁰, F. Eisenhut ⁶³, D. Elia ⁴⁹, B. Erazmus ¹⁰³, F. Ercolessi ²⁵, F. Erhardt ⁸⁹, M.R. Ersdal²⁰, B. Espagnon ⁷², G. Eulisse ³², D. Evans ¹⁰⁰, S. Evdokimov ¹⁴⁰, L. Fabbietti ⁹⁵, M. Faggin ²⁷, J. Faivre ⁷³, F. Fan ⁶, W. Fan ⁷⁴, A. Fantoni ⁴⁸, M. Fasel ⁸⁷, P. Fedichio²⁹, A. Feliciello ⁵⁵, G. Feofilov ¹⁴⁰, A. Fernández Téllez ⁴⁴, L. Ferrandi ¹¹⁰, M.B. Ferrer ³², A. Ferrero ¹²⁸, C. Ferrero ⁵⁵, A. Ferretti ²⁴, V.J.G. Feuillard ⁹⁴, V. Filova ³⁵, D. Finogeev ¹⁴⁰, F.M. Fionda ⁵¹, F. Flor ¹¹⁴, A.N. Flores ¹⁰⁸, S. Foertsch ⁶⁷, I. Fokin ⁹⁴, S. Fokin ¹⁴⁰, E. Fragiaco ⁵⁶, E. Frajna ¹³⁶, U. Fuchs ³², N. Funicello ²⁸, C. Furget ⁷³, A. Furs ¹⁴⁰, T. Fusayasu ⁹⁸, J.J. Gaardhøje ⁸³, M. Gagliardi ²⁴, A.M. Gago ¹⁰¹, C.D. Galvan ¹⁰⁹, D.R. Gangadharan ¹¹⁴, P. Ganoti ⁷⁸, C. Garabatos ⁹⁷, J.R.A. Garcia ⁴⁴, E. Garcia-Solis ⁹, K. Garg ¹⁰³, C. Gargiulo ³², K. Garner¹³⁵, P. Gasik ⁹⁷, A. Gautam ¹¹⁶, M.B. Gay Ducati ⁶⁵, M. Germain ¹⁰³, A. Ghimouz¹²³, C. Ghosh¹³², M. Giacalone ^{50,25}, P. Giubellino ^{97,55}, P. Giubilato ²⁷, A.M.C. Glaenger ¹²⁸, P. Glässel ⁹⁴, E. Glimos ¹²⁰, D.J.Q. Goh ⁷⁶, V. Gonzalez ¹³⁴, L.H. González-Trueba ⁶⁶, M. Gorgon ², S. Gotovac³³, V. Grabski ⁶⁶, L.K. Graczykowski ¹³³, E. Grecka ⁸⁶, A. Grelli ⁵⁸, C. Grigoras ³², V. Grigoriev ¹⁴⁰, S. Grigoryan ^{141,1}, F. Grosa ³², J.F. Grosse-Oetringhaus ³², R. Grosso ⁹⁷, D. Grund ³⁵, G.G. Guardiano ¹¹¹, R. Guernane ⁷³, M. Guilbaud ¹⁰³, K. Gulbrandsen ⁸³, T. Gundem ⁶³, T. Gunji ¹²², W. Guo ⁶,

A. Gupta ⁹¹, R. Gupta ⁹¹, S.P. Guzman ⁴⁴, L. Gyulai ¹³⁶, M.K. Habib ⁹⁷, C. Hadjidakis ⁷²,
 F.U. Haider ⁹¹, H. Hamagaki ⁷⁶, A. Hamdi ⁷⁴, M. Hamid ⁶, Y. Han ¹³⁸, R. Hannigan ¹⁰⁸,
 M.R. Haque ¹³³, J.W. Harris ¹³⁷, A. Harton ⁹, H. Hassan ⁸⁷, D. Hatzifotiadou ⁵⁰, P. Hauer ⁴²,
 L.B. Havener ¹³⁷, S.T. Heckel ⁹⁵, E. Hellbär ⁹⁷, H. Helstrup ³⁴, M. Hemmer ⁶³, T. Herman ³⁵,
 G. Herrera Corral ⁸, F. Herrmann ¹³⁵, S. Herrmann ¹²⁶, K.F. Hetland ³⁴, B. Heybeck ⁶³,
 H. Hillemanns ³², C. Hills ¹¹⁷, B. Hippolyte ¹²⁷, F.W. Hoffmann ⁶⁹, B. Hofman ⁵⁸, B. Hohlweger ⁸⁴,
 G.H. Hong ¹³⁸, M. Horst ⁹⁵, A. Horzyk ², R. Hosokawa ¹⁴, Y. Hou ⁶, P. Hristov ³², C. Hughes ¹²⁰,
 P. Huhn ⁶³, L.M. Huhta ¹¹⁵, C.V. Hulse ⁷², T.J. Humanic ⁸⁸, A. Hutson ¹¹⁴, D. Hutter ³⁸, J.P. Iddon ¹¹⁷,
 R. Ilkaev ¹⁴⁰, H. Ilyas ¹³, M. Inaba ¹²³, G.M. Innocenti ³², M. Ippolitov ¹⁴⁰, A. Isakov ⁸⁶, T. Isidori ¹¹⁶,
 M.S. Islam ⁹⁹, M. Ivanov ¹², M. Ivanov ⁹⁷, V. Ivanov ¹⁴⁰, M. Jablonski ², B. Jacak ⁷⁴, N. Jacazio ³²,
 P.M. Jacobs ⁷⁴, S. Jadlovská ¹⁰⁶, J. Jadlovsky ¹⁰⁶, S. Jaelani ⁸², L. Jaffe ³⁸, C. Jahnke ¹¹¹,
 M.J. Jakubowska ¹³³, M.A. Janik ¹³³, T. Janson ⁶⁹, M. Jercic ⁸⁹, S. Jia ¹⁰, A.A.P. Jimenez ⁶⁴, F. Jonas ⁸⁷,
 J.M. Jowett ^{32,97}, J. Jung ⁶³, M. Jung ⁶³, A. Junique ³², A. Jusko ¹⁰⁰, M.J. Kabus ^{32,133}, J. Kaewjai ¹⁰⁵,
 P. Kalinak ⁵⁹, A.S. Kalteyer ⁹⁷, A. Kalweit ³², V. Kaplin ¹⁴⁰, A. Karasu Uysal ⁷¹, D. Karatovic ⁸⁹,
 O. Karavichev ¹⁴⁰, T. Karavicheva ¹⁴⁰, P. Karczmarczyk ¹³³, E. Karpechev ¹⁴⁰, U. Keschull ⁶⁹,
 R. Keidel ¹³⁹, D.L.D. Keijdener ⁵⁸, M. Keil ³², B. Ketzer ⁴², A.M. Khan ⁶, S. Khan ¹⁵,
 A. Khanzadeev ¹⁴⁰, Y. Kharlov ¹⁴⁰, A. Khatun ^{116,15}, A. Khuntia ¹⁰⁷, M.B. Kidson ¹¹³, B. Kileng ³⁴,
 B. Kim ¹⁶, C. Kim ¹⁶, D.J. Kim ¹¹⁵, E.J. Kim ⁶⁸, J. Kim ¹³⁸, J.S. Kim ⁴⁰, J. Kim ⁶⁸, M. Kim ^{18,94},
 S. Kim ¹⁷, T. Kim ¹³⁸, K. Kimura ⁹², S. Kirsch ⁶³, I. Kisel ³⁸, S. Kiselev ¹⁴⁰, A. Kisiel ¹³³,
 J.P. Kitowski ², J.L. Klay ⁵, J. Klein ³², S. Klein ⁷⁴, C. Klein-Bösing ¹³⁵, M. Kleiner ⁶³,
 T. Klemenz ⁹⁵, A. Kluge ³², A.G. Knospe ¹¹⁴, C. Kobdaj ¹⁰⁵, T. Kollegger ⁹⁷, A. Kondratyev ¹⁴¹,
 N. Kondratyeva ¹⁴⁰, E. Kondratyuk ¹⁴⁰, J. König ⁶³, S.A. Königstorfer ⁹⁵, P.J. Konopka ³²,
 G. Kornakov ¹³³, S.D. Koryciak ², A. Kotliarov ⁸⁶, V. Kovalenko ¹⁴⁰, M. Kowalski ¹⁰⁷,
 V. Kozuharov ³⁶, I. Králik ⁵⁹, A. Kravčáková ³⁷, L. Kreis ⁹⁷, M. Krivda ^{100,59}, F. Krizek ⁸⁶,
 K. Krizkova Gajdosova ³⁵, M. Kroesen ⁹⁴, M. Krüger ⁶³, D.M. Krupova ³⁵, E. Kryshen ¹⁴⁰,
 V. Kučera ³², C. Kuhn ¹²⁷, P.G. Kuijper ⁸⁴, T. Kumaoka ¹²³, D. Kumar ¹³², L. Kumar ⁹⁰, N. Kumar ⁹⁰,
 S. Kumar ³¹, S. Kundu ³², P. Kurashvili ⁷⁹, A. Kurepin ¹⁴⁰, A.B. Kurepin ¹⁴⁰, A. Kuryakin ¹⁴⁰,
 S. Kuschpil ⁸⁶, J. Kvapil ¹⁰⁰, M.J. Kweon ⁵⁷, J.Y. Kwon ⁵⁷, Y. Kwon ¹³⁸, S.L. La Pointe ³⁸, P. La
 Rocca ²⁶, Y.S. Lal ⁷⁴, A. Lakrathok ¹⁰⁵, M. Lamanna ³², R. Langoy ¹¹⁹, P. Larionov ³², E. Laudi ³²,
 L. Lautner ^{32,95}, R. Lavicka ¹⁰², T. Lazareva ¹⁴⁰, R. Lea ^{131,54}, H. Lee ¹⁰⁴, G. Legras ¹³⁵,
 J. Lehrbach ³⁸, R.C. Lemmon ⁸⁵, I. León Monzón ¹⁰⁹, M.M. Lesch ⁹⁵, E.D. Lesser ¹⁸, M. Lettrich ⁹⁵,
 P. Lévai ¹³⁶, X. Li ¹⁰, X.L. Li ⁶, J. Lien ¹¹⁹, R. Lietava ¹⁰⁰, I. Likmeta ¹¹⁴, B. Lim ^{24,16}, S.H. Lim ¹⁶,
 V. Lindenstruth ³⁸, A. Lindner ⁴⁵, C. Lippmann ⁹⁷, A. Liu ¹⁸, D.H. Liu ⁶, J. Liu ¹¹⁷, I.M. Lofnes ²⁰,
 C. Loizides ⁸⁷, S. Lokos ¹⁰⁷, J. Lomker ⁵⁸, P. Loncar ³³, J.A. Lopez ⁹⁴, X. Lopez ¹²⁵, E. López
 Torres ⁷, P. Lu ^{97,118}, J.R. Luhder ¹³⁵, M. Lunardon ²⁷, G. Luparello ⁵⁶, Y.G. Ma ³⁹, A. Maevskaya ¹⁴⁰,
 M. Mager ³², T. Mahmoud ⁴², A. Maire ¹²⁷, M.V. Makariev ³⁶, M. Malaev ¹⁴⁰, G. Malfattore ²⁵,
 N.M. Malik ⁹¹, Q.W. Malik ¹⁹, S.K. Malik ⁹¹, L. Malinina ^{VII,141}, D. Mal'Kevich ¹⁴⁰, D. Mallick ⁸⁰,
 N. Mallick ⁴⁷, G. Mandaglio ^{30,52}, V. Manko ¹⁴⁰, F. Manso ¹²⁵, V. Manzari ⁴⁹, Y. Mao ⁶,
 G.V. Margagliotti ²³, A. Margotti ⁵⁰, A. Marín ⁹⁷, C. Markert ¹⁰⁸, P. Martinengo ³², J.L. Martinez ¹¹⁴,
 M.I. Martínez ⁴⁴, G. Martínez García ¹⁰³, S. Masciocchi ⁹⁷, M. Maserà ²⁴, A. Masoni ⁵¹,
 L. Massacrier ⁷², A. Mastroserio ^{129,49}, O. Matonoha ⁷⁵, P.F.T. Matuoka ¹¹⁰, A. Matyja ¹⁰⁷, C. Mayer ¹⁰⁷,
 A.L. Mazuecos ³², F. Mazzaschi ²⁴, M. Mazzilli ³², J.E. Mdhuli ¹²¹, A.F. Mechler ⁶³, Y. Melikyan ^{43,140},
 A. Menchaca-Rocha ⁶⁶, E. Meninno ^{102,28}, A.S. Menon ¹¹⁴, M. Meres ¹², S. Mhlanga ^{113,67}, Y. Miake ¹²³,
 L. Micheletti ⁵⁵, L.C. Migliorin ¹²⁶, D.L. Mihaylov ⁹⁵, K. Mikhaylov ^{141,140}, A.N. Mishra ¹³⁶,
 D. Miśkowiec ⁹⁷, A. Modak ⁴, A.P. Mohanty ⁵⁸, B. Mohanty ⁸⁰, M. Mohisin Khan ^{V,15},
 M.A. Molander ⁴³, Z. Moravcova ⁸³, C. Mordasini ⁹⁵, D.A. Moreira De Godoy ¹³⁵, I. Morozov ¹⁴⁰,
 A. Morsch ³², T. Mrnjavac ³², V. Muccifora ⁴⁸, S. Muhuri ¹³², J.D. Mulligan ⁷⁴, A. Mulliri ²²,
 M.G. Munhoz ¹¹⁰, R.H. Munzer ⁶³, H. Murakami ¹²², S. Murray ¹¹³, L. Musa ³², J. Musinsky ⁵⁹,
 J.W. Myrcha ¹³³, B. Naik ¹²¹, A.I. Nambrath ¹⁸, B.K. Nandi ⁴⁶, R. Nania ⁵⁰, E. Nappi ⁴⁹,
 A.F. Nassirpour ⁷⁵, A. Nath ⁹⁴, C. Nattrass ¹²⁰, M.N. Naydenov ³⁶, A. Neagu ¹⁹, A. Negru ¹²⁴,
 L. Nellen ⁶⁴, S.V. Nesbo ³⁴, G. Neskovic ³⁸, D. Nesterov ¹⁴⁰, B.S. Nielsen ⁸³, E.G. Nielsen ⁸³,
 S. Nikolaev ¹⁴⁰, S. Nikulin ¹⁴⁰, V. Nikulin ¹⁴⁰, F. Noferini ⁵⁰, S. Noh ¹¹, P. Nomokonov ¹⁴¹,
 J. Norman ¹¹⁷, N. Novitzky ¹²³, P. Nowakowski ¹³³, A. Nyanin ¹⁴⁰, J. Nystrand ²⁰, M. Ogino ⁷⁶,
 A. Ohlson ⁷⁵, V.A. Okorokov ¹⁴⁰, J. Oleniacz ¹³³, A.C. Oliveira Da Silva ¹²⁰, M.H. Oliver ¹³⁷,
 A. Onnerstad ¹¹⁵, C. Oppedisano ⁵⁵, A. Ortiz Velasquez ⁶⁴, J. Otwinowski ¹⁰⁷, M. Oya ⁹², K. Oyama ⁷⁶,
 Y. Pachmayer ⁹⁴, S. Padhan ⁴⁶, D. Pagano ^{131,54}, G. Paic ⁶⁴, A. Palasciano ⁴⁹, S. Panebianco ¹²⁸,

H. Park¹²³, H. Park¹⁰⁴, J. Park⁵⁷, J.E. Parkkila³², R.N. Patra⁹¹, B. Paul²², H. Pei⁶,
T. Peitzmann⁵⁸, X. Peng⁶, M. Pennisi²⁴, L.G. Pereira⁶⁵, D. Peresunko¹⁴⁰, G.M. Perez⁷,
S. Perrin¹²⁸, Y. Pestov¹⁴⁰, V. Petráček³⁵, V. Petrov¹⁴⁰, M. Petrovici⁴⁵, R.P. Pezzi^{103,65}, S. Piano⁵⁶,
M. Pikna¹², P. Pillot¹⁰³, O. Pinazza^{50,32}, L. Pinsky¹¹⁴, C. Pinto⁹⁵, S. Pisano⁴⁸, M. Płoskoń⁷⁴,
M. Planinic⁸⁹, F. Pliquett⁶³, M.G. Poghosyan⁸⁷, B. Polichtchouk¹⁴⁰, S. Politano²⁹, N. Poljak⁸⁹,
A. Pop⁴⁵, S. Porteboeuf-Houssais¹²⁵, V. Pozdniakov¹⁴¹, K.K. Pradhan⁴⁷, S.K. Prasad⁴, S. Prasad⁴⁷,
R. Preghenella⁵⁰, F. Prino⁵⁵, C.A. Pruneau¹³⁴, I. Pshenichnov¹⁴⁰, M. Puccio³², S. Pucillo²⁴,
Z. Pugelova¹⁰⁶, S. Qiu⁸⁴, L. Quaglia²⁴, R.E. Quishpe¹¹⁴, S. Ragoni^{14,100}, A. Rakotozafindrabe¹²⁸,
L. Ramello^{130,55}, F. Rami¹²⁷, S.A.R. Ramirez⁴⁴, T.A. Rancien⁷³, M. Rasa²⁶, S.S. Räsänen⁴³,
R. Rath⁵⁰, M.P. Rauch²⁰, I. Ravasenga⁸⁴, K.F. Read^{87,120}, C. Reckziegel¹¹², A.R. Redelbach³⁸,
K. Redlich^{71,79}, C.A. Reetz⁹⁷, A. Rehman²⁰, F. Reidt³², H.A. Reme-Ness³⁴, Z. Rescakova³⁷,
K. Reygiers⁹⁴, A. Riabov¹⁴⁰, V. Riabov¹⁴⁰, R. Ricci²⁸, M. Richter¹⁹, A.A. Riedel⁹⁵,
W. Riegler³², C. Ristea⁶², M. Rodríguez Cahuantzi⁴⁴, K. Røed¹⁹, R. Rogalev¹⁴⁰, E. Rogochaya¹⁴¹,
T.S. Rogoschinski⁶³, D. Rohr³², D. Röhrich²⁰, P.F. Rojas⁴⁴, S. Rojas Torres³⁵, P.S. Rokita¹³³,
G. Romanenko¹⁴¹, F. Ronchetti⁴⁸, A. Rosano^{30,52}, E.D. Rosas⁶⁴, K. Roslon¹³³, A. Rossi⁵³,
A. Roy⁴⁷, S. Roy⁴⁶, N. Rubini²⁵, O.V. Rueda^{114,75}, D. Ruggiano¹³³, R. Rui²³, B. Rumyantsev¹⁴¹,
P.G. Russek², R. Russo⁸⁴, A. Rustamov⁸¹, E. Ryabinkin¹⁴⁰, Y. Ryabov¹⁴⁰, A. Rybicki¹⁰⁷,
H. Rytkonen¹¹⁵, W. Rzesa¹³³, O.A.M. Saarimaki⁴³, R. Sadek¹⁰³, S. Sadhu³¹, S. Sadovsky¹⁴⁰,
J. Saetre²⁰, K. Šafařík³⁵, S.K. Saha⁴, S. Saha⁸⁰, B. Sahoo⁴⁶, R. Sahoo⁴⁷, S. Sahoo⁶⁰, D. Sahu⁴⁷,
P.K. Sahu⁶⁰, J. Saini¹³², K. Sajdakova³⁷, S. Sakai¹²³, M.P. Salvan⁹⁷, S. Sambyal⁹¹, I. Sanna^{32,95},
T.B. Saramela¹¹⁰, D. Sarkar¹³⁴, N. Sarkar¹³², P. Sarma⁴¹, V. Sarritzu²², V.M. Sarti⁹⁵, M.H.P. Sas¹³⁷,
J. Schambach⁸⁷, H.S. Scheid⁶³, C. Schiaua⁴⁵, R. Schicker⁹⁴, A. Schmäh⁹⁴, C. Schmidt⁹⁷,
H.R. Schmidt⁹³, M.O. Schmidt³², M. Schmidt⁹³, N.V. Schmidt⁸⁷, A.R. Schmier¹²⁰, R. Schotter¹²⁷,
A. Schröter³⁸, J. Schukraft³², K. Schwarz⁹⁷, K. Schweda⁹⁷, G. Scioli²⁵, E. Scomparin⁵⁵,
J.E. Seger¹⁴, Y. Sekiguchi¹²², D. Sekihata¹²², I. Selyuzhenkov^{97,140}, S. Senyukov¹²⁷, J.J. Seo⁵⁷,
D. Serebryakov¹⁴⁰, L. Šerkšnytė⁹⁵, A. Sevcenco⁶², T.J. Shaba⁶⁷, A. Shabetai¹⁰³, R. Shahoyan³²,
A. Shangaraev¹⁴⁰, A. Sharma⁹⁰, B. Sharma⁹¹, D. Sharma⁴⁶, H. Sharma¹⁰⁷, M. Sharma⁹¹,
S. Sharma⁷⁶, S. Sharma⁹¹, U. Sharma⁹¹, A. Shatat⁷², O. Sheibani¹¹⁴, K. Shigaki⁹², M. Shimomura⁷⁷,
J. Shin¹¹, S. Shirinkin¹⁴⁰, Q. Shou³⁹, Y. Sibiriak¹⁴⁰, S. Siddhanta⁵¹, T. Siemiarczuk⁷⁹, T.F. Silva¹¹⁰,
D. Silvermyr⁷⁵, T. Simantathammakul¹⁰⁵, R. Simeonov³⁶, B. Singh⁹¹, B. Singh⁹⁵, R. Singh⁸⁰,
R. Singh⁹¹, R. Singh⁴⁷, S. Singh¹⁵, V.K. Singh¹³², V. Singhal¹³², T. Sinha⁹⁹, B. Sitar¹²,
M. Sitta^{130,55}, T.B. Skaali¹⁹, G. Skorodumovs⁹⁴, M. Slupecki⁴³, N. Smirnov¹³⁷, R.J.M. Snellings⁵⁸,
E.H. Solheim¹⁹, J. Song¹¹⁴, A. Songmoonak¹⁰⁵, F. Soramel²⁷, R. Spijkers⁸⁴, I. Sputowska¹⁰⁷,
J. Staa⁷⁵, J. Stachel⁹⁴, I. Stan⁶², P.J. Steffanic¹²⁰, S.F. Stiefelmaier⁹⁴, D. Stocco¹⁰³,
I. Storehaug¹⁹, P. Stratmann¹³⁵, S. Strazzi²⁵, C.P. Stylianidis⁸⁴, A.A.P. Suaide¹¹⁰, C. Suire⁷²,
M. Sukhanov¹⁴⁰, M. Suljic³², R. Sultanov¹⁴⁰, V. Sumberia⁹¹, S. Sumowidagdo⁸², S. Swain⁶⁰,
I. Szarka¹², M. Szymkowski¹³³, S.F. Taghavi⁹⁵, G. Taillepiéd⁹⁷, J. Takahashi¹¹¹, G.J. Tambave²⁰,
S. Tang^{125,6}, Z. Tang¹¹⁸, J.D. Tapia Takaki¹¹⁶, N. Tapus¹²⁴, L.A. Tarasovicova¹³⁵, M.G. Tartzila⁴⁵,
G.F. Tassielli³¹, A. Tauro³², G. Tejeda Muñoz⁴⁴, A. Telesca³², L. Terlizzi²⁴, C. Terrevoli¹¹⁴,
G. Tersimonov³, S. Thakur⁴, D. Thomas¹⁰⁸, A. Tikhonov¹⁴⁰, A.R. Timmins¹¹⁴, M. Tkacik¹⁰⁶,
T. Tkacik¹⁰⁶, A. Toia⁶³, R. Tokumoto⁹², N. Topilskaya¹⁴⁰, M. Toppi⁴⁸, F. Torres-Acosta¹⁸,
T. Tork⁷², A.G. Torres Ramos³¹, A. Trifiró^{30,52}, A.S. Triolo^{30,52}, S. Tripathy⁵⁰, T. Tripathy⁴⁶,
S. Trogolo³², V. Trubnikov³, W.H. Trzaska¹¹⁵, T.P. Trzcinski¹³³, A. Tumkin¹⁴⁰, R. Turrisi⁵³,
T.S. Tveter¹⁹, K. Ullaland²⁰, B. Ulukutlu⁹⁵, A. Uras¹²⁶, M. Urioni^{54,131}, G.L. Usai²², M. Vala³⁷,
N. Valle²¹, L.V.R. van Doremalen⁵⁸, M. van Leeuwen⁸⁴, C.A. van Veen⁹⁴, R.J.G. van Weelden⁸⁴,
P. Vande Vuyve³², D. Varga¹³⁶, Z. Varga¹³⁶, M. Vasileiou⁷⁸, A. Vasiliev¹⁴⁰, O. Vázquez Doce⁴⁸,
V. Vechernin¹⁴⁰, E. Vercellin²⁴, S. Vergara Limón⁴⁴, L. Vermunt⁹⁷, R. Vértesi¹³⁶, M. Verweij⁵⁸,
L. Vickovic³³, Z. Vilakazi¹²¹, O. Villalobos Baillie¹⁰⁰, A. Villani²³, G. Vino⁴⁹, A. Vinogradov¹⁴⁰,
T. Virgili²⁸, V. Vislavicius⁷⁵, A. Vodopyanov¹⁴¹, B. Volkel³², M.A. Völkl⁹⁴, K. Voloshin¹⁴⁰,
S.A. Voloshin¹³⁴, G. Volpe³¹, B. von Haller³², I. Vorobyev⁹⁵, N. Vozniuk¹⁴⁰, J. Vrláková³⁷,
C. Wang³⁹, D. Wang³⁹, Y. Wang³⁹, A. Wegrzynek³², F.T. Weiglhofer³⁸, S.C. Wenzel³²,
J.P. Wessels¹³⁵, S.L. Weyhmiller¹³⁷, J. Wiechula⁶³, J. Wikne¹⁹, G. Wilk⁷⁹, J. Wilkinson⁹⁷,
G.A. Willems¹³⁵, B. Windelband⁹⁴, M. Winn¹²⁸, J.R. Wright¹⁰⁸, W. Wu³⁹, Y. Wu¹¹⁸, R. Xu⁶,
A. Yadav⁴², A.K. Yadav¹³², S. Yalcin⁷¹, Y. Yamaguchi⁹², S. Yang²⁰, S. Yano⁹², Z. Yin⁶,
I.-K. Yoo¹⁶, J.H. Yoon⁵⁷, S. Yuan²⁰, A. Yuncu⁹⁴, V. Zaccolo²³, C. Zampolli³², F. Zanone⁹⁴,
N. Zardoshti^{32,100}, A. Zarochentsev¹⁴⁰, P. Závada⁶¹, N. Zaviyalov¹⁴⁰, M. Zhalov¹⁴⁰, B. Zhang⁶,

L. Zhang ³⁹, S. Zhang ³⁹, X. Zhang ⁶, Y. Zhang¹¹⁸, Z. Zhang ⁶, M. Zhao ¹⁰, V. Zherebchevskii ¹⁴⁰,
Y. Zhi¹⁰, D. Zhou ⁶, Y. Zhou ⁸³, J. Zhu ^{97,6}, Y. Zhu⁶, S.C. Zugravel ⁵⁵, N. Zurlo ^{131,54}

Affiliation Notes

^I Deceased

^{II} Also at: Max-Planck-Institut für Physik, Munich, Germany

^{III} Also at: Italian National Agency for New Technologies, Energy and Sustainable Economic Development (ENEA), Bologna, Italy

^{IV} Also at: Dipartimento DET del Politecnico di Torino, Turin, Italy

^V Also at: Department of Applied Physics, Aligarh Muslim University, Aligarh, India

^{VI} Also at: Institute of Theoretical Physics, University of Wrocław, Poland

^{VII} Also at: An institution covered by a cooperation agreement with CERN

Collaboration Institutes

¹ A.I. Alikhanyan National Science Laboratory (Yerevan Physics Institute) Foundation, Yerevan, Armenia

² AGH University of Science and Technology, Cracow, Poland

³ Bogolyubov Institute for Theoretical Physics, National Academy of Sciences of Ukraine, Kiev, Ukraine

⁴ Bose Institute, Department of Physics and Centre for Astroparticle Physics and Space Science (CAPSS), Kolkata, India

⁵ California Polytechnic State University, San Luis Obispo, California, United States

⁶ Central China Normal University, Wuhan, China

⁷ Centro de Aplicaciones Tecnológicas y Desarrollo Nuclear (CEADEN), Havana, Cuba

⁸ Centro de Investigación y de Estudios Avanzados (CINVESTAV), Mexico City and Mérida, Mexico

⁹ Chicago State University, Chicago, Illinois, United States

¹⁰ China Institute of Atomic Energy, Beijing, China

¹¹ Chungbuk National University, Cheongju, Republic of Korea

¹² Comenius University Bratislava, Faculty of Mathematics, Physics and Informatics, Bratislava, Slovak Republic

¹³ COMSATS University Islamabad, Islamabad, Pakistan

¹⁴ Creighton University, Omaha, Nebraska, United States

¹⁵ Department of Physics, Aligarh Muslim University, Aligarh, India

¹⁶ Department of Physics, Pusan National University, Pusan, Republic of Korea

¹⁷ Department of Physics, Sejong University, Seoul, Republic of Korea

¹⁸ Department of Physics, University of California, Berkeley, California, United States

¹⁹ Department of Physics, University of Oslo, Oslo, Norway

²⁰ Department of Physics and Technology, University of Bergen, Bergen, Norway

²¹ Dipartimento di Fisica, Università di Pavia, Pavia, Italy

²² Dipartimento di Fisica dell'Università and Sezione INFN, Cagliari, Italy

²³ Dipartimento di Fisica dell'Università and Sezione INFN, Trieste, Italy

²⁴ Dipartimento di Fisica dell'Università and Sezione INFN, Turin, Italy

²⁵ Dipartimento di Fisica e Astronomia dell'Università and Sezione INFN, Bologna, Italy

²⁶ Dipartimento di Fisica e Astronomia dell'Università and Sezione INFN, Catania, Italy

²⁷ Dipartimento di Fisica e Astronomia dell'Università and Sezione INFN, Padova, Italy

²⁸ Dipartimento di Fisica 'E.R. Caianiello' dell'Università and Gruppo Collegato INFN, Salerno, Italy

²⁹ Dipartimento DISAT del Politecnico and Sezione INFN, Turin, Italy

³⁰ Dipartimento di Scienze MIFT, Università di Messina, Messina, Italy

³¹ Dipartimento Interateneo di Fisica 'M. Merlin' and Sezione INFN, Bari, Italy

³² European Organization for Nuclear Research (CERN), Geneva, Switzerland

³³ Faculty of Electrical Engineering, Mechanical Engineering and Naval Architecture, University of Split, Split, Croatia

³⁴ Faculty of Engineering and Science, Western Norway University of Applied Sciences, Bergen, Norway

³⁵ Faculty of Nuclear Sciences and Physical Engineering, Czech Technical University in Prague, Prague, Czech Republic

³⁶ Faculty of Physics, Sofia University, Sofia, Bulgaria

³⁷ Faculty of Science, P.J. Šafárik University, Košice, Slovak Republic

- ³⁸ Frankfurt Institute for Advanced Studies, Johann Wolfgang Goethe-Universität Frankfurt, Frankfurt, Germany
- ³⁹ Fudan University, Shanghai, China
- ⁴⁰ Gangneung-Wonju National University, Gangneung, Republic of Korea
- ⁴¹ Gauhati University, Department of Physics, Guwahati, India
- ⁴² Helmholtz-Institut für Strahlen- und Kernphysik, Rheinische Friedrich-Wilhelms-Universität Bonn, Bonn, Germany
- ⁴³ Helsinki Institute of Physics (HIP), Helsinki, Finland
- ⁴⁴ High Energy Physics Group, Universidad Autónoma de Puebla, Puebla, Mexico
- ⁴⁵ Horia Hulubei National Institute of Physics and Nuclear Engineering, Bucharest, Romania
- ⁴⁶ Indian Institute of Technology Bombay (IIT), Mumbai, India
- ⁴⁷ Indian Institute of Technology Indore, Indore, India
- ⁴⁸ INFN, Laboratori Nazionali di Frascati, Frascati, Italy
- ⁴⁹ INFN, Sezione di Bari, Bari, Italy
- ⁵⁰ INFN, Sezione di Bologna, Bologna, Italy
- ⁵¹ INFN, Sezione di Cagliari, Cagliari, Italy
- ⁵² INFN, Sezione di Catania, Catania, Italy
- ⁵³ INFN, Sezione di Padova, Padova, Italy
- ⁵⁴ INFN, Sezione di Pavia, Pavia, Italy
- ⁵⁵ INFN, Sezione di Torino, Turin, Italy
- ⁵⁶ INFN, Sezione di Trieste, Trieste, Italy
- ⁵⁷ Inha University, Incheon, Republic of Korea
- ⁵⁸ Institute for Gravitational and Subatomic Physics (GRASP), Utrecht University/Nikhef, Utrecht, Netherlands
- ⁵⁹ Institute of Experimental Physics, Slovak Academy of Sciences, Košice, Slovak Republic
- ⁶⁰ Institute of Physics, Homi Bhabha National Institute, Bhubaneswar, India
- ⁶¹ Institute of Physics of the Czech Academy of Sciences, Prague, Czech Republic
- ⁶² Institute of Space Science (ISS), Bucharest, Romania
- ⁶³ Institut für Kernphysik, Johann Wolfgang Goethe-Universität Frankfurt, Frankfurt, Germany
- ⁶⁴ Instituto de Ciencias Nucleares, Universidad Nacional Autónoma de México, Mexico City, Mexico
- ⁶⁵ Instituto de Física, Universidade Federal do Rio Grande do Sul (UFRGS), Porto Alegre, Brazil
- ⁶⁶ Instituto de Física, Universidad Nacional Autónoma de México, Mexico City, Mexico
- ⁶⁷ iThemba LABS, National Research Foundation, Somerset West, South Africa
- ⁶⁸ Jeonbuk National University, Jeonju, Republic of Korea
- ⁶⁹ Johann-Wolfgang-Goethe Universität Frankfurt Institut für Informatik, Fachbereich Informatik und Mathematik, Frankfurt, Germany
- ⁷⁰ Korea Institute of Science and Technology Information, Daejeon, Republic of Korea
- ⁷¹ KTO Karatay University, Konya, Turkey
- ⁷² Laboratoire de Physique des 2 Infinis, Irène Joliot-Curie, Orsay, France
- ⁷³ Laboratoire de Physique Subatomique et de Cosmologie, Université Grenoble-Alpes, CNRS-IN2P3, Grenoble, France
- ⁷⁴ Lawrence Berkeley National Laboratory, Berkeley, California, United States
- ⁷⁵ Lund University Department of Physics, Division of Particle Physics, Lund, Sweden
- ⁷⁶ Nagasaki Institute of Applied Science, Nagasaki, Japan
- ⁷⁷ Nara Women's University (NWU), Nara, Japan
- ⁷⁸ National and Kapodistrian University of Athens, School of Science, Department of Physics, Athens, Greece
- ⁷⁹ National Centre for Nuclear Research, Warsaw, Poland
- ⁸⁰ National Institute of Science Education and Research, Homi Bhabha National Institute, Jatni, India
- ⁸¹ National Nuclear Research Center, Baku, Azerbaijan
- ⁸² National Research and Innovation Agency - BRIN, Jakarta, Indonesia
- ⁸³ Niels Bohr Institute, University of Copenhagen, Copenhagen, Denmark
- ⁸⁴ Nikhef, National institute for subatomic physics, Amsterdam, Netherlands
- ⁸⁵ Nuclear Physics Group, STFC Daresbury Laboratory, Daresbury, United Kingdom
- ⁸⁶ Nuclear Physics Institute of the Czech Academy of Sciences, Husinec-Řež, Czech Republic
- ⁸⁷ Oak Ridge National Laboratory, Oak Ridge, Tennessee, United States
- ⁸⁸ Ohio State University, Columbus, Ohio, United States
- ⁸⁹ Physics department, Faculty of science, University of Zagreb, Zagreb, Croatia
- ⁹⁰ Physics Department, Panjab University, Chandigarh, India

- ⁹¹ Physics Department, University of Jammu, Jammu, India
- ⁹² Physics Program and International Institute for Sustainability with Knotted Chiral Meta Matter (SKCM2), Hiroshima University, Hiroshima, Japan
- ⁹³ Physikalisches Institut, Eberhard-Karls-Universität Tübingen, Tübingen, Germany
- ⁹⁴ Physikalisches Institut, Ruprecht-Karls-Universität Heidelberg, Heidelberg, Germany
- ⁹⁵ Physik Department, Technische Universität München, Munich, Germany
- ⁹⁶ Politecnico di Bari and Sezione INFN, Bari, Italy
- ⁹⁷ Research Division and ExtreMe Matter Institute EMMI, GSI Helmholtzzentrum für Schwerionenforschung GmbH, Darmstadt, Germany
- ⁹⁸ Saga University, Saga, Japan
- ⁹⁹ Saha Institute of Nuclear Physics, Homi Bhabha National Institute, Kolkata, India
- ¹⁰⁰ School of Physics and Astronomy, University of Birmingham, Birmingham, United Kingdom
- ¹⁰¹ Sección Física, Departamento de Ciencias, Pontificia Universidad Católica del Perú, Lima, Peru
- ¹⁰² Stefan Meyer Institut für Subatomare Physik (SMI), Vienna, Austria
- ¹⁰³ SUBATECH, IMT Atlantique, Nantes Université, CNRS-IN2P3, Nantes, France
- ¹⁰⁴ Sungkyunkwan University, Suwon City, Republic of Korea
- ¹⁰⁵ Suranaree University of Technology, Nakhon Ratchasima, Thailand
- ¹⁰⁶ Technical University of Košice, Košice, Slovak Republic
- ¹⁰⁷ The Henryk Niewodniczanski Institute of Nuclear Physics, Polish Academy of Sciences, Cracow, Poland
- ¹⁰⁸ The University of Texas at Austin, Austin, Texas, United States
- ¹⁰⁹ Universidad Autónoma de Sinaloa, Culiacán, Mexico
- ¹¹⁰ Universidade de São Paulo (USP), São Paulo, Brazil
- ¹¹¹ Universidade Estadual de Campinas (UNICAMP), Campinas, Brazil
- ¹¹² Universidade Federal do ABC, Santo Andre, Brazil
- ¹¹³ University of Cape Town, Cape Town, South Africa
- ¹¹⁴ University of Houston, Houston, Texas, United States
- ¹¹⁵ University of Jyväskylä, Jyväskylä, Finland
- ¹¹⁶ University of Kansas, Lawrence, Kansas, United States
- ¹¹⁷ University of Liverpool, Liverpool, United Kingdom
- ¹¹⁸ University of Science and Technology of China, Hefei, China
- ¹¹⁹ University of South-Eastern Norway, Kongsberg, Norway
- ¹²⁰ University of Tennessee, Knoxville, Tennessee, United States
- ¹²¹ University of the Witwatersrand, Johannesburg, South Africa
- ¹²² University of Tokyo, Tokyo, Japan
- ¹²³ University of Tsukuba, Tsukuba, Japan
- ¹²⁴ University Politehnica of Bucharest, Bucharest, Romania
- ¹²⁵ Université Clermont Auvergne, CNRS/IN2P3, LPC, Clermont-Ferrand, France
- ¹²⁶ Université de Lyon, CNRS/IN2P3, Institut de Physique des 2 Infinis de Lyon, Lyon, France
- ¹²⁷ Université de Strasbourg, CNRS, IPHC UMR 7178, F-67000 Strasbourg, France, Strasbourg, France
- ¹²⁸ Université Paris-Saclay Centre d'Etudes de Saclay (CEA), IRFU, Département de Physique Nucléaire (DPhN), Saclay, France
- ¹²⁹ Università degli Studi di Foggia, Foggia, Italy
- ¹³⁰ Università del Piemonte Orientale, Vercelli, Italy
- ¹³¹ Università di Brescia, Brescia, Italy
- ¹³² Variable Energy Cyclotron Centre, Homi Bhabha National Institute, Kolkata, India
- ¹³³ Warsaw University of Technology, Warsaw, Poland
- ¹³⁴ Wayne State University, Detroit, Michigan, United States
- ¹³⁵ Westfälische Wilhelms-Universität Münster, Institut für Kernphysik, Münster, Germany
- ¹³⁶ Wigner Research Centre for Physics, Budapest, Hungary
- ¹³⁷ Yale University, New Haven, Connecticut, United States
- ¹³⁸ Yonsei University, Seoul, Republic of Korea
- ¹³⁹ Zentrum für Technologie und Transfer (ZTT), Worms, Germany
- ¹⁴⁰ Affiliated with an institute covered by a cooperation agreement with CERN
- ¹⁴¹ Affiliated with an international laboratory covered by a cooperation agreement with CERN.